WILEY | Hindawi

Research Article

Performance Analysis of Cognitive SWIPT Ergodic Capacity Based on Different Selection Policies

Shilong Cao,[1] **Fei Lin** (ID)**,**[2] **and Jiemei Liu**[2]

[1]*School of Electrical Engineering and Automation, Qilu University of Technology (Shandong Academy of Sciences), Jinan, China*
[2]*School of Information and Automation Engineering, Qilu University of Technology (Shandong Academy of Sciences), Jinan, China*

Correspondence should be addressed to Fei Lin; linfei@qlu.edu.cn

The advent of 5G era and the increase of terminal's numbers have led to increasing demand for spectrum resources and energy simultaneously. Therefore, this paper studies how to combine the cognitive radio (CR) and the Simultaneous Wireless Information and Power Transfer (SWIPT) technology effectively in a multiuser scenario, in which the spectrum utilization and energy efficiency are both improved. Firstly, the system model is designed of above cognitive SWIPT system, in which the cognitive users (CU) can choose spectrum access policy based on the amount of data transmission of licensed user. And then, according to cognitive users' channel conditions and forwarding power, a concept of trust value and different relay selection policies is proposed. Subsequently, the according system ergodic capacity is analyzed. Finally, simulation results of system performance are provided to validate the analytical results. It shows that cognitive SWIPT technology can improve the system ergodic capacity and the spectrum access opportunities of cognitive users effectively, thereby improving the efficiency of energy and spectrum utilization.

1. Introduction

With the commercialization of 5G technology, the explosive growth of the number of terminals is an inevitable trend. How to deal with the resulting shortage of spectrum and increase in energy consumption is the focus of attention of scholars.

After the concepts of cognitive radio (CR) and Simultaneous Wireless Information and Power Transfer (SWIPT) that were proposed by Moitla [1] and Varshney [2], respectively, many scholars try to combine the two technologies together and find according application scenario.

The core idea of CR is that the licensed user (LU) and cognitive user (CU) may share one spectrum band simultaneously. As a combination, cognitive SWIPT can make full use of spectrum resources and achieve simultaneous transmission of information and energy, thus improving the utilization efficiency of spectrum and energy simultaneously.

In [3, 4], two papers mainly studied outage performance and bit error rate but did not consider the model of cognitive SWIPT. In the cognitive SWIPT system, [5] analyzed the cognitive transmitter's throughput and according upper in cognitive radio network (CRN) but did not study the spectrum access policy of energy harvesting (EH) cognitive radio network. So, in [6], the CU can harvest energy from the LU and access the authorized spectrum in underlay manner, but only one-way relay is considered in the model. That is, the CU only assists the LU to send information and does not transmit its own information. [7] considered a cognitive SWIPT transmission process and gave the outage performance analysis but did not consider the interference problem of cognitive relay to LU. [8] aims to achieve fairness among CUs in IoT cooperative NOMA-based CR transmission. They design a power allocation algorithm, an independent battery constraint at each node is considered, and power gap among transmissions of two NOMA users is applied for successive interference cancellation. However, this document does not consider the combination of SWIPT and CR and the relevant polices of relay selection. [9] considers a cooperative relaying system (CRS) empowered by SWIPT and nonorthogonal multiple access (NOMA) where

SWIPT and NOMA are implemented for their energy and spectral efficiencies, respectively. Then, they analyze error performance and the diversity performance of the CRS-SWIPT-NOMA under Nakagami-m fading channels. Different from the [9], we analyze the system capacity under Rayleigh fading channels.

Therefore, this paper designed a hybrid cognitive SWIPT system in which has multiple potential cognitive relays, and the LU will be regarded as in heavy load case and light one in terms of the amount of data transmission [10, 11]. In heavy load case, the selected cognitive relay node needs to harvest energy from LU's transmitted signal and then adopts amplify and forward (AF) protocol with the part of harvesting energy to forward the LU's information. In light load case, the selected cognitive relay gets the opportunity to access the spectrum with underlay mode to transmit its own information with the rest power. When the LU is in idle mode, the cognitive relay can fully use the spectrum. And then, according to cognitive users' channel conditions and forwarding power, a concept of trust value and different relay selection policies is proposed. Subsequently, the according system ergodic capacity is analyzed. Finally, simulation results of system performance are provided to validate the analytical results. It shows that cognitive SWIPT technology can improve the system ergodic capacity and the spectrum access opportunities of cognitive users effectively, thereby improving the efficiency of energy and spectrum utilization.

2. System Model

The system model is shown in Figure 1,which combines CR with SWIPT technologies together. It is assumed that each terminal has an antenna. In detail, S is the licensed transmitter sending data to fusion node D, and R_i represents the i-th CU; that is, cognitive relay that was equipped with EH devices. Every R_i may be the volunteer to assist data transmission of LU.

When the LU is in different load states, R_i will use different access methods to share the spectrum with the LU, as shown in Figure 2. When the LU is in heavy load, R_i adopts the overlay mode to take out part of its own power to assist the LU to forward, thereby offsetting part of the interference to the LU [12]. When LU is in light load, R_i accesses the spectrum in underlay mode to obtain its own data transmission opportunity. At this time, R_i's power is strictly limited to prevent interference to LU.

This paper assumes that all R_i can use SWIPT technology for EH. According to the comprehensive consideration of the fading channel and the forwarding power of R_i, the trust value is proposed in (10). The LU selects an optimal R_i according to the trust value, and the R_i needs to assist LU's communication. At the same time, it is assumed that all R_i have obtained initial energy through EH or manual initialization.

As shown in Figure 1, S sends the signal to the cognitive relay R_i and the destination D at the same time. The whole communication process is divided into two phases. In the first phase, S broadcasts its signal through the direct path

to D and the relay path to R_i. In the second phase, R_i amplifies and forwards the processed signal to D.

In order to obtain energy and information from RF signals and then forward them, the methods of collecting wireless energy mainly include integrated receiver and separated receiver. Integrated energy acquisition can make circuit equipment separate energy signal and information signal from RF signal, but too idealization limits its application. When energy and information are transmitted in parallel, separated energy acquisition uses two receivers to receive energy and information signals, respectively. This technique is widely used because it is easy to implement.

The methods based on separated energy acquisition mainly include power segmentation (PS) and time switching (TS). The two receiver architectures and transfer blocks are shown in Figures 3 and 4.

In Figure 3, h_{SD}, h_{SR_i}, and h_{R_iD} are the channel gains from S to D, S to R_i and R_i to D. N_{R_i} is the noise at the receiving antenna of the R_i. After the power splitter receives the signal transmitted to R_i by the authorized user S, it divides it into two signals for EH and one for information decoding (IR). k is the power split ratio, and $0 < k < 1$, the signal y_{SR_i} is divided into two according to the proportion, and the value of k depends on the actual communication needs. In the PS transmission block of Figure 4, y_{SR_i} is divided into two paths at the same time according to k and lasts for a time T.

In Figure 4, α is the time slot switching factor, and $0 < \alpha < 1$. The transmission block under TS reflects the fundamental difference between TS and PS; that is, after the signal y_{SR_i} is received by R_i, EH and IR are not performed at the same time.

3. Performance Analysis

In this section, the transmitted signal of S is analyzed, and the concept of trust value and the policy of relay selection is defined. Finally, the ergodic capacity of the system is obtained.

3.1. Analyze the Two-Phase Signal. In the first phase, S transmits signals to the D through the direct path which is expressed as

$$y_{SD} = \sqrt{P_S} h_{SD} X_S + N_{SD}. \tag{1}$$

Signals received at the relay R_i can be written as

$$y_{SR_i} = \sqrt{P_S} h_{SR_i} X_S + N_{R_i}, \tag{2}$$

Where P_S is the transmitting power of the LU, X_S is the transmitted signal of the LU, N_{SD} is the overall channel noise at D including the receive antenna noise and the RF to baseband signal conversion noise, and N_{SD} is modeled as independent complex additive white Gaussian noise (AWGN) with zero mean and variance $N_{0_{SD}}$.
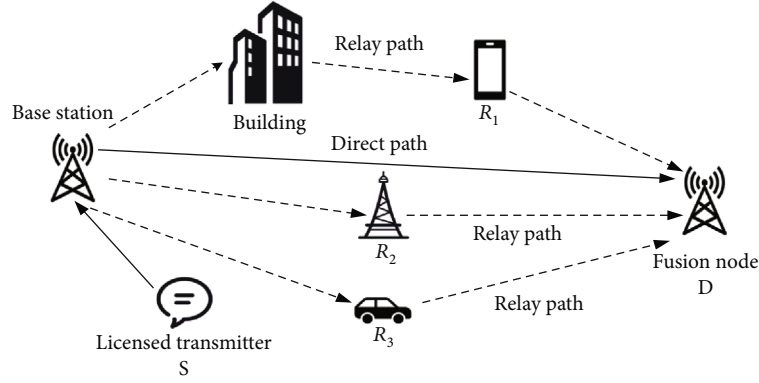
FIGURE 1: System model.
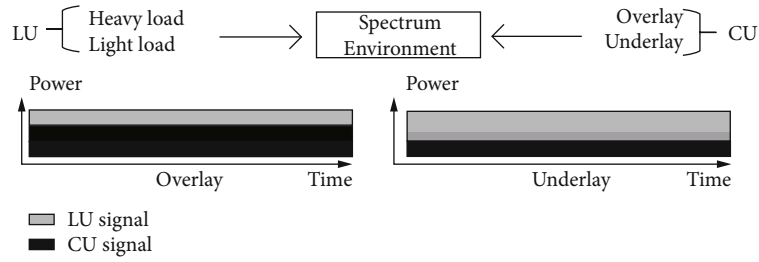
FIGURE 2: Access method.
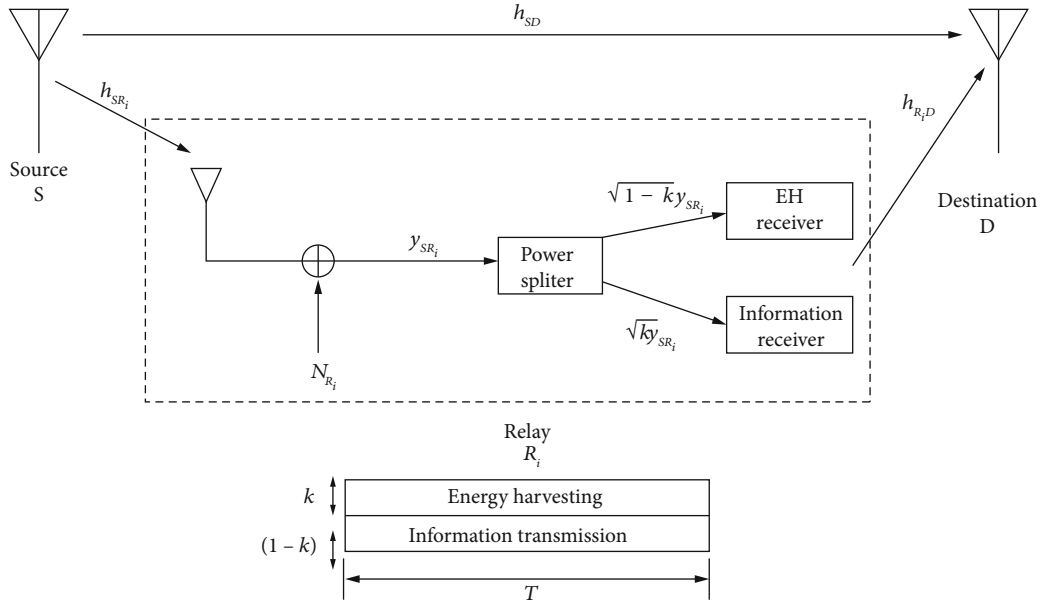
FIGURE 3: PS receiver architecture and transmission block diagram.

Then, the received signal of the IR processing module part is

$$y_{IR} = \sqrt{k}y_{SR_i} + N_{R_iC} = \sqrt{kP_S h_{SR_i} X_S} + \sqrt{kN_{R_i}} + N_{R_iC}, \quad (3)$$

Where N_{R_iC} is the complex AWGN with zero mean and variance $N_{0_{R_iC}}$ due to the conversion of the RF signal to baseband signal at the R_i.

Then, the received signal of the EH processing module part is

$$y_{EH} = \sqrt{1-k}y_{SR_i}. \quad (4)$$
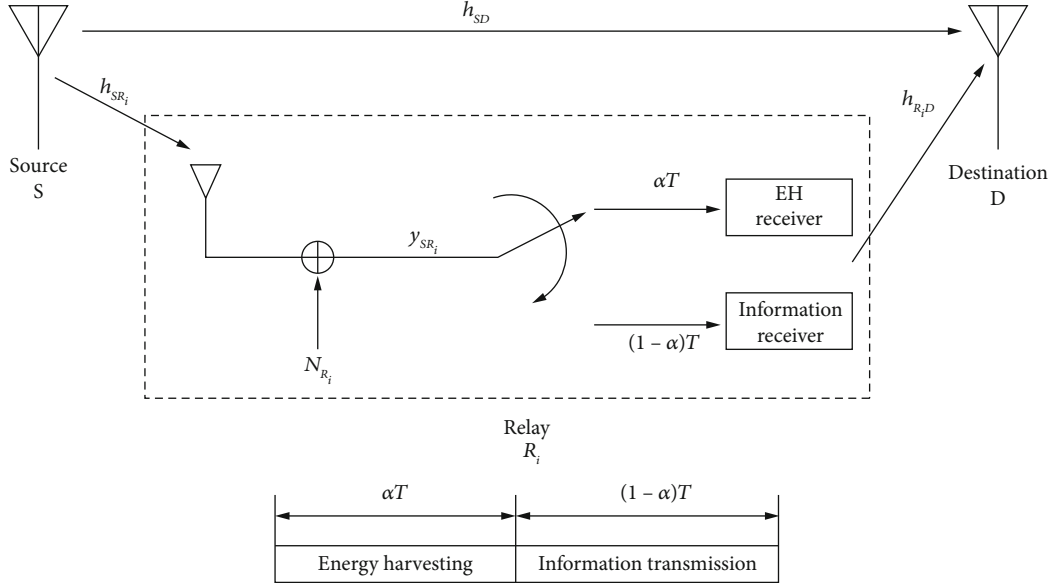
FIGURE 4: TS receiver architecture and transmission block diagram.

TABLE 1: Parameter settings.

Modulation and demodulation mode	QPSK
Power split ratio	0.9
Energy conversion efficiency factor	0.99
Receiving mode of terminal	MRC
Number of CR	10
Range of SNR	-5 : 40 dB
Information transmission rate	100 Mb/S

At the end of phase 1, the available power at R_i is

$$P_{R_i} = \eta(1-k)P_S|h_{SR_i}|^2. \tag{5}$$

η is the energy conversion efficiency factor. In (5),

$$P_{R_i} = P_{\text{part1}} + P_{\text{part2}}. \tag{6}$$

P_{part1} is the power used by R_i to assist LU to transmit information, and P_{part2} is used by R_i to transmit its own information.

In the second phase, R_i uses power P_{part1} to forward the signal in IR, and the required energy is provided by EH. The signal from R_i is

$$X_{R_i} = \sqrt{\frac{P_{\text{Part1}}}{kP_S E\left[|h_{SR_i}|^2\right] + kN_{0_{SR_i}} + N_{0_{R_iC}}}} y_{IR}. \tag{7}$$

$\sqrt{kP_S E[|h_{SR_i}|^2] + kN_{0_{SR_i}} + N_{0_{R_iC}}}$ is the power scaling factor forwarded by AF, and $E[|h_{SR_i}|^2]$ is the expected value of $|h_{SR_i}|^2$.

At the end of phase 2, the signal received from R_i at terminal D is

$$y_{R_iD} = h_{R_iD}X_{R_i} + N_{R_iD}. \tag{8}$$

Substitute (3) and (7) into (8) and further obtain (9):

$$y_{R_iD} = \sqrt{\frac{P_{Part1}kP_S}{kP_S E\left[|h_{SR_i}|^2\right] + kN_{0_{SR_i}} + N_{0_{R_iC}}}} h_{R_iD}h_{SR_i}X_s$$
$$+ \sqrt{\frac{P_{Part1}}{kP_S E\left[|h_{SR_i}|^2\right] + kN_{0_{SR_i}} + N_{0_{R_iC}}}} h_{R_iD}N_{SR_i} + N_{R_iD}. \tag{9}$$

It can be obtained that the total signal received at terminal D after maximum ratio combining (MRC) is $y_D = a_{R_iD} y_{R_iD} + a_{SD}y_{SD}$, where a_{R_iD} and a_{SD} are the MRC weighting coefficient.

3.2. Multirelay Selection Policy Analysis. This paper proposes the concept of trust value when the LU needs to select a CU to forward information in the cognitive SWIPT system. The trust value considers the CU's forwarding power and channel conditions. Above that, two methods of relay selection according to the trust value threshold and the 3σ rule threshold are proposed.

3.2.1. Establishment of Trust Value. This paper proposes a concept of trust value, which is related to the relay-associated channels and the provided power of CU. Assuming that the average SNR of the channel where R_i is located is $E(\gamma_{SR_iD})$, according to (6), the trust value φ_i of R_i is defined

as

$$\varphi_i = \gamma_{\overline{SR_iD}} \frac{P_{\text{part1}}}{P_{R_i}}, i = 1, 2 \cdots n, \qquad (10)$$

where $E(\gamma_{SR_iD}) = \gamma_{\overline{SR_iD}}$, γ_{SR_iD} is the instaneous received SNR about the path $S \longrightarrow R_i \longrightarrow D$.

The trust value φ_i is regarded as the label on the R_i, and the LU can select the appropriate R_i to assist in transmitting by using the φ_i and selection polices.

3.2.2. Threshold-Based Relay Selection Policy. In order to select a suitable cognitive relay, this paper establish the thresholds under the trust values to exclude cognitive users who cannot assist LU.

The threshold is the average of the trust value of each CU, and then one is selected among the CUs greater than the threshold.

The threshold $\bar{\varphi}$ is

$$\bar{\varphi} = E\left[\sum_{n=1}^{i} \varphi_n \right]. \qquad (11)$$

Relative to the threshold of a single value, this paper also using the 3σ principle to determine a threshold range (a, b), which is expressed as

$$\begin{aligned} a &= \text{mean}(\varphi_i) - 3 * \text{std}(\varphi_i), \\ b &= \text{mean}(\varphi_i) + 3 * \text{std}(\varphi_i). \end{aligned} \qquad (12)$$

In statistics, 3σ principle is the percentage within one standard deviation, two standard deviations, and three standard deviations from the average in the normal distribution. The original intention of setting up 3σ principle is to exclude certain malicious users. Such malicious users are considered to be as follows: in order to participate in assisting the LU to transmit information, improve their performance abnormally to obtain the first priority of transmission and thus carry out eavesdropping. However, the 3σ principle will exclude users who have abnormal φ_i and are not in the range of (a, b).

3.3. Instantaneous Receiving SNR Analysis. From equation (1), we can get the instantaneous receiving SNR of the direct path $S \longrightarrow D$

$$\gamma_{SD} = \frac{P_S |h_{SD}|^2}{N_{0_{SD}}}. \qquad (13)$$

According to (9), the instantaneous receiving SNR of the path $S \longrightarrow R_i \longrightarrow D$ can be obtained by using a method sim-

ilar to [3].

$$\begin{aligned} \gamma_{SR_iD} &= \frac{\left(P_{Part1} |h_{R_iD}|^2 / N_{0_{R_iD}} \right) \cdot \left(k P_S |h_{SR_i}|^2 / N_{0_{SR_i}} \right)}{\left(P_{Part1} |h_{R_iD}|^2 / N_{0_{R_iD}} \right) + \left(k P_S E\left[|h_{SR_i}|^2 \right] / N_{0_{SR_i}} \right) + 1} \\ &= \frac{\gamma_{R_iD} \cdot \gamma_{SR_i}}{\gamma_{R_iD} + \bar{\gamma}_{SR_i} + 1}. \end{aligned} \qquad (14)$$

In (14), $\bar{\gamma}_{SR_i} = E[\gamma_{SR_i}], N_{0_{R_iD}}$, is the variance of N_{R_iD}, and $N_{SR_i} = \sqrt{k} N_{R_i} + N_{R_iC}$ can be obtained from equations (3) and (9). There are two different points between equation (14) and SNR formula in [3, 4], one is that the CU does not use the full power for forwarding, but a part of the total power, and the other is we assumed that the direct path and the relay path are independent of each other.

In (14),

$$\begin{aligned} \gamma_{SR_i} &= \frac{k P_S |h_{SR_i}|^2}{N_{0_{SR_i}}}, \\ \gamma_{R_iD} &= \frac{P_{Part1} |h_{R_iD}|^2}{N_{0_{R_iD}}}. \end{aligned} \qquad (15)$$

Then, the SNR is the exponential distribution with the parameter (16).

$$\lambda_{SD} = \frac{N_{0_{SD}}}{P_S \sigma_{SD}^2}. \qquad (16)$$

The probability density function (PDF) is

$$p(\lambda_{SD}) = \begin{cases} \lambda_{SD} e^{-\lambda_{SD} x}, x > 0 \\ 0, \text{other} \end{cases}. \qquad (17)$$

The PDF of equation (14) is derived from [3].

$$\begin{aligned} p\left(\gamma_{SR_iD} \right) &= \frac{2}{\bar{\gamma}_{SR_i} \bar{\gamma}_{R_iD}} \exp\left(-\frac{\gamma_{SR_iD}}{\bar{\gamma}_{SR_i}} \right) \int_0^\infty I d\gamma_{R_iD} \\ &\quad + \frac{2\left(\bar{\gamma}_{SR_i} + 1 \right)}{\bar{\gamma}_{SR_i} \bar{\gamma}_{R_iD}} \exp\left(-\frac{\gamma_{SR_iD}}{\bar{\gamma}_{SR_i}} \right) \int_0^\infty \frac{1}{\gamma_{R_iD}} I d\gamma_{R_iD}, \end{aligned} \qquad (18)$$

where $I = \exp\left(\gamma_{SR_iD}(\gamma_{SR_i} + 1) / \gamma_{SR_i} \gamma_{R_iD} \right) K_0 \left(\sqrt[2]{(\gamma_{R_iD} / \bar{\gamma}_{R_iD})} \right)$, and K_0 represents the second zero-order modified Bessel function. Using the Meijer-G function [13–15], the formula
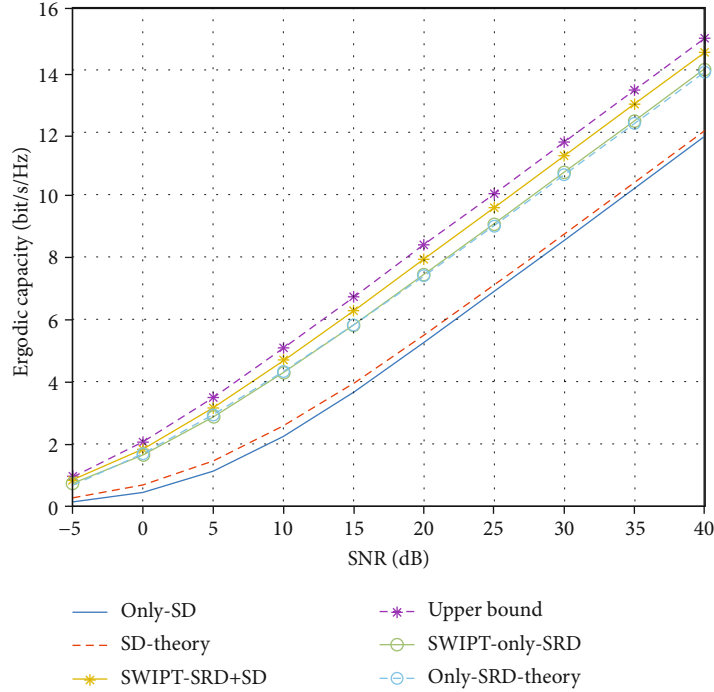
FIGURE 5: Comparison between the theoretical analysis and the simulated results.
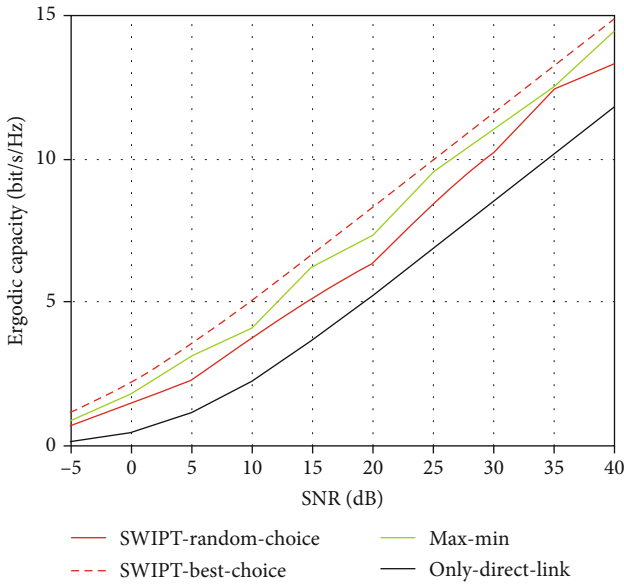
FIGURE 6: The capacity analysis without threshold.

(18) can be expressed as

$$
\begin{aligned}
p\left(\gamma_{SR_iD}\right) = & \frac{1}{\bar{\gamma}_{SR_i}} \exp\left(-\frac{\gamma_{SR_iD}}{\bar{\gamma}_{SR_i}}\right) G_{0,3}^{3,0}\left(\frac{\beta\gamma_{SR_iD}}{\bar{\gamma}_{SR_i}\gamma_{R_iD}}\,\bigg|\,\begin{matrix}[\{1\},\{\quad\}]\\ [\{0,1,1\},\{\quad\}]\end{matrix}\right) \\
& + \frac{\beta}{\bar{\gamma}_{SR_i}\gamma_{R_iD}} \exp\left(-\frac{\gamma_{SR_iD}}{\bar{\gamma}_{SR_i}}\right) G_{0,3}^{3,0}\left(\frac{\beta\gamma_{SR_iD}}{\bar{\gamma}_{SR_i}\gamma_{R_iD}}\,\bigg|\,\begin{matrix}[\{\quad\},\{\quad\}]\\ [\{0,0,0\},\{\}]\end{matrix}\right).
\end{aligned}
$$

$$(19)$$

In (19), $\beta = (\bar{\gamma}_{SR_i} + 1)$, $\bar{\gamma}_{R_iD} = P_{Part1}E[|h_{R_iD}|^2]/N_{0_{R_iD}}$.

Because of the complexity of equation (19), it is hard to achieve a simply expression of 's distribution.

3.4. System Ergodic Capacity Analysis. When there is only a direct path $S \longrightarrow D$, the system ergodic capacity of LU is

$$
C_{SD} = E[log_2(1 + \gamma)] = \int_0^\infty log_2(1 + x)p(\gamma_{SD})dx. \quad (20)
$$

From the Meijer-G function, (20) can also be expressed as

$$
C_{SD} = \frac{\lambda_{SD}}{\ln(2)} G_{2,3}^{3,1}\left(x\,\bigg|\,\begin{matrix}[\{-1\},\{0\}]\\ [\{-1,-10\},\{\}]\end{matrix}\right). \quad (21)
$$

See the Appendix for the certification process.

3.4.1. When LU Is in Heavy Load. As discussed in II, the LU selected a CU as a relay in heavy load; so, the ergodic capacity can be written as

$$
C_{Heavy} = E[log_2(1 + \gamma_t)], \quad (22)
$$

where $\gamma_t = \gamma_{SD} + \gamma_{SR_iD}$. In order to achieve the closed form expression about (22), we should use the pdf of γ_t which is hard to analyze.
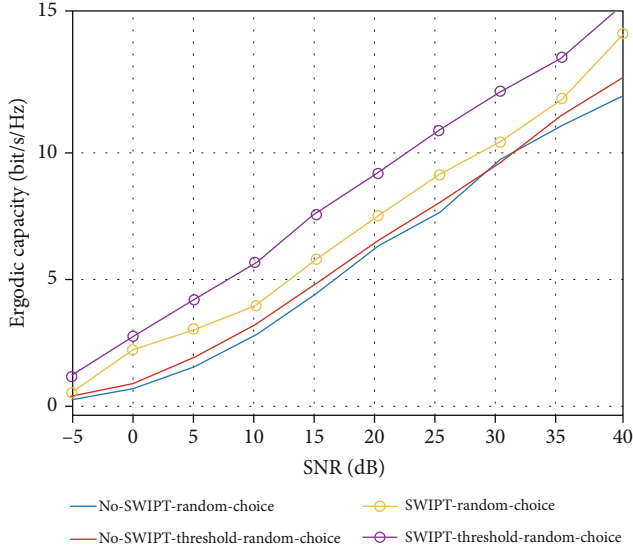
FIGURE 7: The capacity analysis base on the trust value threshold.
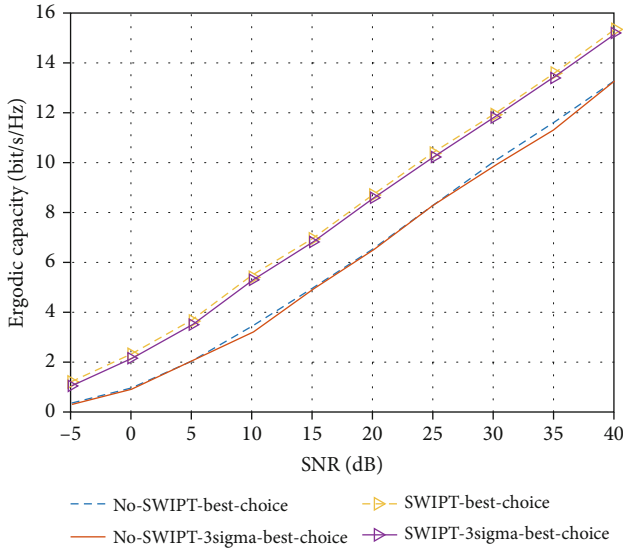
FIGURE 8: The capacity analysis based on the 3σ principle threshold.

When there is only a relay path $S \longrightarrow R_i \longrightarrow D$, the system ergodic capacity of LU can be obtained by (14)

$$
\begin{aligned}
C_{SR_iD} &= \int_0^\infty log_2(1+y)p\left(\gamma_{SR_iD}\right)dy \\
&= \int_0^\infty log_2(1+y)\left[\frac{2}{\bar{\gamma}_{SR_i}\bar{\gamma}_{R_iD}} \exp\left(-\frac{\gamma_{SR_iD}y}{\bar{\gamma}_{SR_i}}\right)\int_0^\infty Id\gamma_{R_iD}\right. \\
&\left.+ \frac{2\left(\bar{\gamma}_{SR_i}+1\right)}{\bar{\gamma}_{SR_i}\bar{\gamma}_{R_iD}} \exp\left(-\frac{\gamma_{SR_iD}y}{\bar{\gamma}_{SR_i}}\right)\int_0^\infty \frac{1}{\gamma_{R_iD}}Id\gamma_{R_iD}\right]dx.
\end{aligned}
$$
(23)

From (20) and (22), the theoretical equation of system

ergodic ability when LU is under heavy load is

$$
\begin{aligned}
C_{\text{Heavy}} &= E\left[log_2\left(1+\gamma_{SD}+\gamma_{SR_iD}\right)\right] \\
&= \int_0^\infty \int_0^\infty log_2(1+x+y)p(\gamma_{SD})p\left(\gamma_{SR_iD}\right)dxdy,
\end{aligned}
$$
(24)

$$
= \int_0^\infty \int_0^\infty log_2(1+x+y)\cdot\gamma_{SD}e^{-\gamma_{SD}\cdot x-a}\cdot\left(\begin{array}{c}aG_{0,3}^{3,0}\left(by\left|\begin{array}{c}[\{1\},\{\ \}]\\ [\{0,1,1\},\{\ \}]\end{array}\right.\right)\\ +bG_{0,3}^{3,0}\left(by\left|\begin{array}{c}[\{\ \},\{\ \}]\\ [\{0,0,0\},\{\ \}]\end{array}\right.\right)\end{array}\right)dxdy.
$$
(25)

In (25), $a = 1/\bar{\gamma}_{SR_i}$, and $b = \beta/\bar{\gamma}_{SR_i}\bar{\gamma}_{R_iD}$.

With Jensen's inequality [16], the ergodic capacity can be simplified as

$$
C_{\text{Heavy}} \le log_2\left(1+E[\gamma_{SD}]+E\left[\gamma_{SR_iD}\right]\right) = log_2\left(1+\bar{\gamma}_{SD}+\bar{\gamma}_{SR_iD}\right).
$$
(26)

3.4.2. When LU Is in Light Load. R_i uses the underlay method to share spectrum with LU and transmits its own information. In this paper, the transmission power P_{part2} of sending its own data is regarded as interference to LU; so, LU's signal to interference plus noise ratio (SINR) can be defined as

$$
\text{SINR} = \frac{P_S}{N_{0_{SD}}+P_{\text{part2}}}\cdot|h_{SD}|^2.
$$
(27)

The interference of R_i to LU must be limited within a certain threshold; so, the requirements are

$$
E[\text{SINR}] = E\left[\frac{P_S}{N_{0_{SD}}+P_{\text{part2}}}\cdot|h_{SD}|^2\right] \ge \gamma_{\text{th}}.
$$
(28)

In (27), γ_{th} is the minimum threshold of the mean value of SINR, which is regarded as a constant. Therefore,

$$
\frac{P_S}{N_{0_{SD}}+P_{\text{part2}}}\sigma_{SD}^2 \ge \gamma_{\text{th}}.
$$
(29)

There are restrictions on the size of P_{part2}, which requires

$$
P_{\text{part2}} \le \frac{P_S\sigma_{SD}^2}{\gamma_{th}} - N_{0_{SD}}.
$$
(30)

4. Simulation Performance Analysis

This chapter analyzes the ergodic capacity of the system using different policies of relay selection when the LU is in different load modes based on the multi-relay situation.

Some parameter settings in the simulation are shown in Table 1.

4.1. Capacity Analysis in Heavy Load. Time spent by the LU to transmit information is defined as T, the QPSK
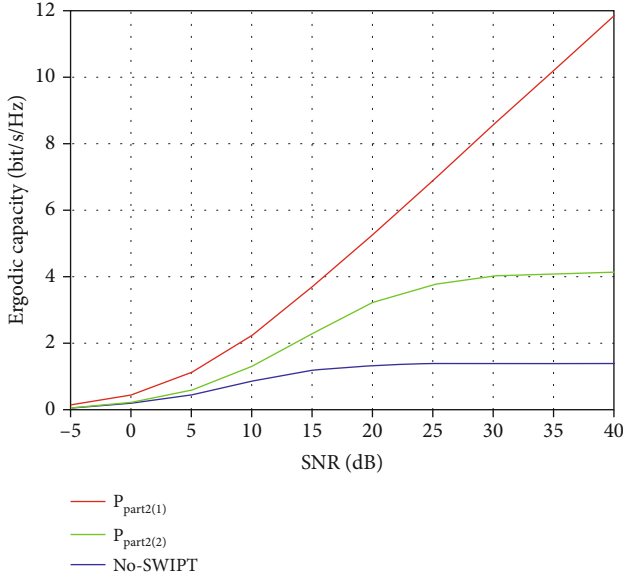
FIGURE 9: The impact of the P_{part2} on the ergodic capacity of the LU.
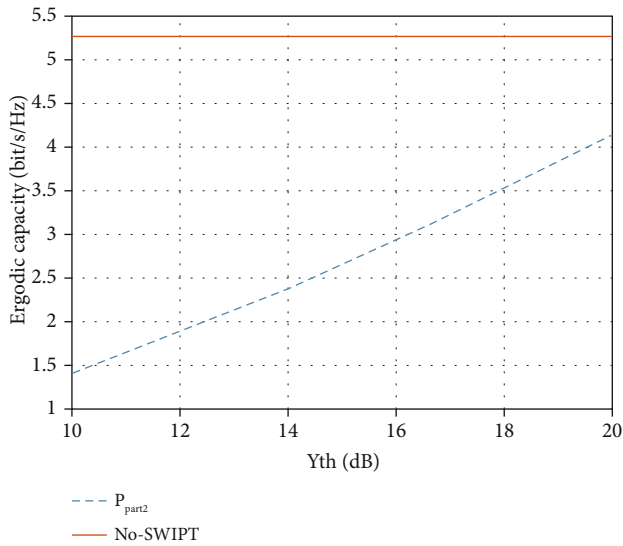
FIGURE 10: The impact of the threshold on the ergodic capacity of the LU.

modulation is used, and the power split ratio k is 0.9. This paper compares the simulation results and theoretical analysis of each path firstly. Then, different relay selection policies are compared according to the Trust Value.

Figure 5 shows the comparison between theoretical analysis and simulation results. It can be seen that the theoretical analysis and simulation results are basically consistent when there is only direct path $S \longrightarrow D$, only relay path $S \longrightarrow R \longrightarrow D$ or both cases in the system model, which proves the reliability of the theoretical analysis in this paper.

Without threshold, the optimal selection policy is to select the relay with the largest trust value. The simulation curves of ergodic capacity of the two policies are shown in Figure 6.

It can be seen from Figure 6 that the capacity of the optimal relay selection policy without threshold is higher than the policy of random relay selection, and both are higher than the system without SWIPT technology. This policy can be applied to simple small-scale networks, and relays with different performance can be selected to assist in forwarding information according to the needs of different communication systems.

In addition, Figure 6 also compares the traditional Max-Min method. It can be seen that the Max-Min method is not as good as the optimal selection policy based on trust value. This is because the Max-Min method can dynamically ensure the communication quality of the channel with poor channel conditions, but it has not developed and utilized the best communication path of the system, and the reliability of channel transmission still needs to be improved.

The system ergodic capacity under the policy of multirelay random selection according to the trust value threshold in (11) is shown in Figure 7.

Figure 7 also is a random selection policy, with the restriction of the threshold value added. The system ergodic capacity is significantly higher than the capacity without the threshold value in Figure 6. In actual communication scenarios, the establishment of the threshold value can screen out a batch of high-quality relays for multiple LU, thereby improving the efficiency of relay selection.

In Figure 8, under the threshold limit established based on the 3σ principle, the capacity under the optimal relay selection policy is very similar to the capacity established without threshold. In addition, due to the limitation of 3σ principle, some users with abnormal trust values are excluded. The original intention of this policy is to exclude some malicious users who falsely improve their own parameters to obtain the highest trust value.

4.2. Capacity Analysis in Light Load. The R_i can share the spectrum with LU in underlay mode and transmit its own information by using the remaining energy which is harvesting by LU's signal. The power P_{part2} of CU will be strictly limited in (29). This is determined by the core idea of CR and the underlay method.

Figures 9 and 10 reflect the impact of the P_{part2} and threshold on the ergodic capacity of the LU when the LU is under light load, respectively.

In Figure 9, $P_{part2(1)} > P_{part2(2)}$, which means the higher the interference to the LU, the lower the capacity. It can be understood that if there are multiple cognitive relays in the system that need to share the spectrum with the LU to transmit their own information, the capacity of the LU will be adversely affected. Therefore, the number of cognitive relay shared with the LU spectrum should be strictly limited.

In Figure 10, the specified SNR is 20 dB. It can be seen from the Figure 9 that when the CU adopts the underlay mode to share the spectrum with the LU, P_{part2} decreases as the threshold increases, and the system ergodic capacity of increases. When there is no relay to occupy spectrum of LU, the system ergodic capacity remains basically unchanged.

5. Conclusion

The different policies of relay selection proposed in this paper can effectively improve the ergodic capacity of the system and have practical application significance. If a user is under heavy load for a long time, SWIPT technology greatly increases the user's system ergodic capacity, and cognitive relay can also use SWIPT to harvest energy. If a user is under light load for a long time, the cognitive relay can share spectrum with the user to transmit its own information and only need to limit its own interference. So, the cognitive SWIPT is a win-win technology.

Some works can be further studied. The final expression of the system ergodic capacity is too complex. How to get a more simplified expression of the final capacity is the next research direction. In addition, how to ensure secure communication in cognitive SWIPT is also a focus of future research.

Appendix

Proof of the Equation (21)

From (17) and (20),

$$
\begin{aligned}
C_{SD} = E[\log(1+\gamma)] &= \int_0^\infty \log_2(1+x)\exp(-\gamma_{SD}x)dx \\
&= \int_0^\infty \log_2(1+x)\exp(-\gamma_{SD}x)dx.
\end{aligned} \tag{A.1}
$$

From the bottom-changing formula, we further get

$$
= \frac{1}{\ln(2)}\int_0^\infty \ln(1+x)\exp(-\gamma_{SD}x)dx. \tag{A.2}
$$

By Meijer-G function [14–16],

$$
\begin{aligned}
&= \frac{1}{\ln(2)}\int_0^\infty G_{2,2}^{1,2}\left(x\left|\begin{matrix}[\{1,1\},\{\ \ \}]\\ [\{1\},\{0\}]\end{matrix}\right.\right) G_{0,1}^{1,0}\left(-\gamma_{SD}x\left|\begin{matrix}[\{\ \},\{\ \ \}]\\ [\{0\},\{\ \ \}]\end{matrix}\right.\right)dx \\
&= \frac{\gamma_{SD}}{\ln(2)} G_{2,3}^{3,1}\left(x\left|\begin{matrix}[\{-1\},\{0\}]\\ [\{-1-10\},\{\ \ \}]\end{matrix}\right.\right).
\end{aligned} \tag{A.3}
$$

Data Availability

The [Source Code] data used to support the findings of this study are available from the corresponding author upon request.

Conflicts of Interest

The authors declare that they have no conflicts of interest.

Acknowledgments

References

[1] J. Mitola and G. J. Maquire, "Cognitive radio: making software radios more personal," *IEEE Personal Communications*, vol. 6, no. 4, pp. 13–18, 1999.

[2] L. R. Varshney, "Transporting information and energy simultaneously," in *IEEE International Symposium on Information Theory (ISIT)*, pp. 1612–1616, IEEE, Toronto, ON, Canada, 2008.

[3] L. Mohjazi, S. Muhaidat, and M. Dianati, "Performance analysis of differential modulation in SWIPT cooperative Networks," *IEEE Signal Processing Letters*, vol. 23, no. 5, pp. 620–624, 2016.

[4] Y. Feng, V. C. M. Leung, and F. Ji, "Performance study for SWIPT cooperative communication systems in shadowed Nakagami fading channels," *IEEE Transactions on Wireless Communications*, vol. 17, no. 2, pp. 1199–1211, 2017.

[5] S. Park and D. Hong, "Achievable throughput of energy harvesting cognitive radio Networks," *IEEE Transactions on Wireless Communications*, vol. 13, no. 2, pp. 1010–1022, 2014.

[6] S. Yin, E. Zhang, Z. Qu, L. Yin, and S. Li, "Optimal cooperation strategy in cognitive radio systems with energy Harvesting," *IEEE Transactions on Wireless Communications*, vol. 13, no. 9, pp. 4693–4707, 2014.

[7] Z. Wang, Z. Chen, B. Xia, L. Luo, and J. Zhou, "Cognitive relay networks with energy harvesting and information transfer: design, analysis, and optimization," *IEEE Transactions on Wireless Communications*, vol. 15, no. 4, pp. 2562–2576, 2016.

[8] Z. Ali, W. U. Khan, S. Sidhu et al., "Fair power allocation in cooperative cognitive systems under NOMA transmission for future IoT networks," *Alexandria Engineering Journal*, vol. 61, no. 1, pp. 575–583, 2022.

[9] F. Kara, "Error performance of cooperative relaying systems empowered by SWIPT and NOMA," *Physical Communication*, vol. 49, p. 101450, 2021.

[10] M. Tao, F. Lin, and Y. Che, "A dynamic matching scheme between licensed user and cognitive User based on deep neural network with Q-learning," in *2019 IEEE 5th International Conference on Computer and Communications (ICCC)*, pp. 1985–1989, 2019.

[11] M. Tao, *Research on Intelligent Spectrum Access and Resource Optimization in Cognitive Radio*, Qilu University of Technology, 2020.

[12] X. Zhou, M. Sun, G. Y. Li, and B. H. F. Juang, "Intelligent wireless communications enabled by cognitive radio and machine learning," *China Communications*, vol. 15, no. 12, pp. 16–48, 2018.

[13] *Papoulis, Probability, Random Variables, and Stochastic Processes*, McGraw-Hill, New York, NY, USA, 3rd edition, 1991.

[14] J. G. Proakis, *Digital Communications*, McGraw-Hill, New York, NY, USA, 4th edition, 2000.

[15] P. M. Shankar, *Fading and Shadowing in Wireless Systems*, Springer, New York, NY, USA, 2012.

[16] A. Goldsmith, *Wireless Communications*, the Press of the University of Cambridge, Cambridge, 2005.